HHS Public Access

Author manuscript

AJNR Am J Neuroradiol. Author manuscript; available in PMC 2017 January 01.

Published in final edited form as:

AJNR Am J Neuroradiol. 2016 July ; 37(7): 1209–1215. doi:10.3174/ajnr.A4724.

Quantitative Susceptibility Mapping in Cerebral Cavernous Malformations: Clinical Correlations

Huan Tan[1], **Lingjiao Zhang**[1], **Abdul Ghani Mikati**[1], **Romuald Girard**[1], **Omaditya Khanna**[1], **Maged D. Fam**[1], **Tian Liu**[2], **Yi Wang**[3,4], **Robert R. Edelman**[5,6], **Gregory Christoforidis**[7], and **Issam A. Awad**[1]

[1]Department of Surgery (Neurosurgery), University of Chicago Medicine and Biological Sciences, University of Chicago, Chicago, IL, USA

[2]MedImageMetric LLC, New York, New York, USA

[3]Department of Radiology, Weill Cornell Medical College, New York, NY, USA

[4]Department of Biomedical Engineering, Cornell University, Ithaca, NY, USA

[5]Department of Radiology, NorthShore University HealthSystem, Evanston, IL, USA

[6]Department of Radiology, Feinberg School of Medicine, Northwestern University, Illinois, USA

[7]Department of Radiology, Pritzker School of Medicine, University of Chicago, Chicago, IL, USA

Abstract

Background and Purpose—To correlate lesional iron deposition assessed by quantitative susceptibility mapping (QSM) with clinical and disease features in patients with cerebral cavernous malformations (CCM).

Materials and Methods—This study was approved by the local Institutional Review Boards, and informed consent was obtained from each participant. Patients underwent routine clinical scan in addition to QSM on 3 Tesla systems. Data from 105 patients met inclusion criteria. CCM lesions identified on susceptibility maps were cross-verified by T2 weighted images and differentiated based on prior overt hemorrhage. Mean susceptibility per CCM lesion ($\bar{\chi}_{\text{lesion}}$) was measured to correlate with lesion volume, age at scan, and hemorrhagic history. Temporal rates of change in $\bar{\chi}_{\text{lesion}}$ was evaluated in 33 patients.

Corresponding Author: Huan Tan, PhD, Department of Surgery, Section of Neurosurgery, SBRI J328, 5841 South Maryland Avenue, MC 3026, Chicago, IL 60637, Phone: (773) 702-5775. Fax: (773) 702-3518. htan1@surgery.bsd.uchicago.edu.

DISCLOSURES: Huan Tan—*RELATED : Grant :* The project was funded in part by the Collaborative and Translational Studies Award through the Institute of Translational Medicine at the University of Chicago (UL1 TR000430) and by the Bill and Judy Davis Research Fund in Neurovascular Research* ; *OTHER RELATIONSHIPS:* Drs. Tian Liu and Yi Wang have filed patents related to QSM technology. Dr. Tian Liu is an employee of MedImageMetric LLC in New York City. **Tian Liu—***RELATED : Grant :* MedImagemetric LLC,* Comments : NIH grant 1 R43 EB015293-01 ; *UNRELATED : Patents (planned, pending or issued) :* I'm listed as an inventor on patent applications related to QSM. **Yi Wang—***RELATED : Grant :* NIH R01NS072370* ; *UNRELATED : Patents (planned, pending or issued) :* I am one of the inventors of QSM ; *Stock/Stock Options :* MedImageMetric LLC, Comments : Is interested in QSM commercialization. **Robert Edelman—***UNRELATED : Grants/Grants Pending :* NIH, Siemens Healthcare ; *Patents (planned, pending or issued) :* Noncontrast MR angiography ; *Royalties :* Siemens Healthcare. **Gregory Christoforidis—***RELATED : Grant :* National Institutes of Health.* **Issam Awad—***RELATED : Grant :* NIH/NINDS,* Davis Research Fund in Neurovascular Surgery Research* ; *UNRELATED : Expert Testimony :* Legal expert testimony, unrelated to subject of research ; *Grants/Grants Pending :* NIH/NINDS.*

Results—Average $\bar{\chi}_{lesion}$ per patient was positively correlated with patient age at scan ($p < 0.05$, 4.1% change with each decade of life). CCM lesions with prior overt hemorrhages exhibited higher $\bar{\chi}_{lesion}$ than those without ($p < 0.05$). Changes in $\bar{\chi}_{lesion}$ during 3 – 15 months follow-up period were small in patients without new hemorrhage between the two scans [bias = −0.0003, 95% CI = [−0.06, 0.06]).

Conclusion—The study revealed a positive correlation between mean QSM signal and patient age in CCM lesions, higher mean QSM signal in hemorrhagic lesions, and minimum longitudinal QSM signal change in clinically stable lesions. QSM has the potential to be a novel imaging biomarker supplementing conventional imaging in CCM. The clinical significance of such measures merits further study.

INTRODUCTION

Cerebral cavernous malformation (CCM) is a common hemorrhagic vascular anomaly of the human brain, affecting more than one million Americans [1]. CCM patients are subject to 1–5% annual risk and an estimated 30% or greater lifetime risk of hemorrhage, epilepsy, seizure, and other neurologic sequelae [2–4]. The clinical consequences of CCM remain unpredictable, and currently there is no known treatment to alter the course of this disease besides surgery.

Iron deposition related to hemorrhage within CCM lesions is a recognized hallmark of disease activity [5–7]. Recently, therapeutic changes in lesion burden have been found with experimental drugs in animal models, where a major phenotypic effect of the therapy was the decrease in iron deposition in treated lesions by immunohistochemistry [6]. Lesional iron was therefore hypothesized to be a marker for disease progression and a relevant therapeutic target. It would be essential to determine whether the disease severity and beneficial effect on iron can also be quantified by a method suitable for clinical studies. The current evaluation of CCM disease burden in humans primarily relies on lesion count and size with magnetic resonance imaging (MRI), in great part due to the imaging of susceptibility effects caused by the iron-rich blood breakdown byproducts. Modern MRI techniques such as susceptibility weighted imaging (SWI) [8] can offer accurate lesion counts [9], however lacks the ability to quantify lesional iron deposition, particularly in larger clinically concerning lesions. The continuing investigation of experimental CCM therapies is in need of a quantitative technique for a more accurate and sensitive assessment of outcomes, and a potential biomarker of novel therapies.

Quantitative susceptibility mapping (QSM) is a non-invasive MRI technique that has the potential to estimate lesional iron content by quantifying the magnetic susceptibility of local tissues [10, 11]. The initial feasibility of QSM in CCM was previously demonstrated in a small cohort of patients [12]. Importantly, QSM as a means to quantify lesional iron in CCM was validated by mass spectroscopy using excised human lesion specimens [12]. However, iron burden and its evolution in relation to disease progression have not been established. Novel discoveries relating iron content and the clinical features of the disease, as well as changes in iron accumulation over time will offer valuable information in understanding the disease pathophysiology and assisting in the development of potential interventions.

In this study, we answer those questions by applying QSM to a large cohort of CCM patients as a part of the routine clinical exam. The following hypotheses were tested: 1) The average CCM susceptibility per patient is correlated with age; 2) lesions with previous hemorrhagic events have higher susceptibility; and 3) changes in lesional susceptibility ($\bar{\chi}_{lesion}$) in a short time (less than 2 years) are insignificant in patients who were clinically stable (i.e. asymptomatic, no bleeds); other changes in QSM over time may reflect new bleeding or recovery from hemorrhage. The goal of this study is to extend from the initial feasibility [12] to explore QSM for clinical measure of the disease severity and correlating lesion-specific behaviors during disease progression.

MATERIALS AND METHODS

Study Design

Clinical features of the CCM disease as well as prior lesion behaviors were correlated with QSM derived iron measurements. A sub-cohort of patients underwent serial QSM measurements, and longitudinal assessment of QSM was correlated with clinical lesion behavior in these cases. In addition, QSM was spatially correlated to the T1- and T2-weighted imaging characteristics of lesions based on blood breakdown products. It needs to be pointed out that the iron sources that contribute to the QSM signal are complex. In the context of the preliminary evidence[12] that demonstrated the mean QSM signal was directly proportional to the actual iron concentration in CCM lesions by mass spectroscopy, the terms mean susceptibility and iron concentration will be used interchangeably in the paper.

Patients

This study enrolled 105 consecutive patients (mean age 39 years, range 3 – 76 years) scheduled for routine clinical evaluation and MR imaging for CCM disease from February 2012 to December 2014. Inclusion criteria for enrollment were the presence of known CCM disease and the absence of other unrelated neurologic pathology. The imaging study took place at the University of Chicago (UC) and NorthShore University HealthSystem (NSUHS). Both institutional review boards approved the study and written informed consent was obtained from each patient.

A total of 175 scans including follow-up imaging were performed in the 105 patients. Thirty seven scans (21%) were excluded from the final analysis due to 1) excessive imaging artifacts because of motion and/or medical implants, and 2) the absence of lesion (e.g. the scan occurred after the lesion was resected). As a result, the final analysis included 138 scans from 95 patients (96 scans in 69 patients at UC and 42 scans in 26 patients at NSUHS). Among those 95 patients, 33 (22 at UC and 11 at NSUHS) received at least one follow-up scan. The time between the repeated scans ranged from 91 to 455 days with an average of 359 days.

For cross sectional analyses, the first QSM of those who had multiple scans was used. A clinical summary of the included patients is shown in Table 1.

Imaging Environments and Data Acquisition

Imaging was performed on 3 Tesla MR systems. 69 patients were imaged at UC (Achieva, Philips, Best, Netherlands) with an eight-channel phased-array head coil, while 26 patients were imaged at NSUHS (MAGNETOM Verio, Siemens, Erlangen, Germany) with a twelve-channel phased-array head coil. Follow-up scans for patients were performed on the same units as the their initial visits.

A three-dimensional, T2*-weighted, multi-echo, spoiled gradient echo sequence was used for QSM data acquisition with the following common parameters: 8 echo times (TEs) with uniform spacing; flip angle 15 degrees; parallel acceleration of a factor 2. The following parameters are system specific – Philips Achieva: TE [min, max], [5.6, 51] ms; field of view, 224 mm; acquisition matrix 224×224; slab encoding thickness, 1mm; repetition time, 66 ms. Siemens Verio: TE [min, max], [3.6, 45] ms; field of view, 240 mm; acquisition matrix 256 × 256; slab encoding thickness, 1.5 mm; repetition time, 55 ms.

Data Reconstruction

QSM images were reconstructed using a morphology-enabled dipole inversion algorithm [10, 13], which generates the local susceptibility distribution by inverting the estimated tissue field map with prior information from the magnitude images. The tissue field map was obtained by removing the background field induced by large susceptibility sources (i.e. air/tissue interface) from the field map derived from the GRE phase images [14]. Image reconstruction was performed locally on a dedicated workstation (Intel Core i7 2.7 GHz, 16 GB RAM) with an average processing time of 8 minutes.

Data Analysis

Extraction of clinical parameters—The electronic medical records of the patients were reviewed by one experienced clinician (more than 20 years of experience in the care of CCM) and de-identified clinical information was collected and stored in a database prior to initiating the correlations. Hemorrhage associated with CCM was defined according to the criteria of Al-Shahi, et al. [15]. Briefly, hemorrhage due to CCM requires both acute or subacute onset of symptoms accompanied by imaging evidence of acute or subacute lesional or extralesional hemorrhage. Cases were classified as familial or sporadic based on lesion count, family history, and/or identified mutations using genetic screenings [9, 16].

Inclusion criteria for lesion analysis—Lesions were selected from the 138 scans with acceptable image quality. Since sporadic cases often only contain a solitary lesion, all lesions in sporadic cases were included. In familial cases, the number of lesions can be innumerable with many small punctate lesions. Hence, we only included lesions with a max cross-diameter equal or greater than 5 mm [17] on the corresponding T2 weighted images that were of higher clinical significance. A total of 407 lesions (64 from 64 scans in 39 sporadic patients and 343 from 74 scans in 56 familial patients) were included in the final analysis.

Lesion susceptibility and volume measurements—CCM lesions appeared hyperintense on the QSM maps and were cross verified with SWI and T2 weighted images. Lesion segmentation was performed using the ImageJ software (National Institute of Health,

Bethesda, MD) by experienced scientists and physicians with high intra- and inter-observer consistency demonstrated previously [18]. The final ROI defined for each lesion was three-dimensional by aggregating 2D ROIs cross multiple slices. Mean susceptibility ($\bar{\chi} = \Sigma\chi_{ROI}/N$, where N is the number of pixels within the 3D ROI) was then calculated per lesion ($\bar{\chi}_{lesion}$) and averaged across patient ($\bar{\chi}_{patient}$). Lesion volume was computed as the product of the total number of pixels in the 3D ROI and the voxel size.

Correlation analyses—We performed correlation analysis between $\bar{\chi}_{lesion}$ (proportional to lesional iron concentration [12]) and a set of clinical parameters consisting of patients' basic characteristics and the CCM disease features. Specific parameters from basic characteristics include patient gender and age at scan, which provides estimation for the duration of lesion presence. Often lesion genesis can occur before it becomes symptomatic; we assumed that older patients were more likely to harbor the lesion for a longer duration. Parameters from the disease feature included lesional volume, sporadic versus familial, and hemorrhagic history. In patients with follow-up scans, we assessed changes over time in $\bar{\chi}_{lesion}$ in the same lesions.

Spatial correlation based on conventional MRI features—Spatial correlation of imaging features between QSM and conventional MRI sequences was conducted in 20 randomly selected lesions in our cohort. Each lesion was spatially segmented by an experienced neuroradiologist (more than 20 years of experience), based on the signal intensity on the conventional T1 and T2 weighted images as different blood breakdown products [19]. Four types of blood byproducts were identified, deoxygenated hemoglobin (DH), intra/extra-cellular methemoglobin (ICM/ECM), and hemosiderin. A category of unknown was used to describe all other depositions within the lesion. The susceptibility of each blood byproduct was empirically determined as high (greater than 1.4 ppm), medium (between 0.6 and 1.4 ppm), or low (less than 0.6 ppm). The distribution of susceptibility measurements across different blood types was analyzed.

Statistical Analysis

Pearson's correlation and Student's t-test were applied to explore the correlations and comparisons made between $\bar{\chi}_{lesion}$ and continuous or dichotomous clinical factors, respectively. Bland-Altman plot was used to assess the changes in patients with repeated scans. Receiver operating characteristic (ROC) analysis was applied to express the diagnostic accuracy of QSM identifying lesions with prior hemorrhages in familial CCM cases. Statistical analyses were performed using GraphPad Prism 4 (GraphPad Software, Inc., USA), and all reported p values were two sided and were considered to be statistically significant at $p < 0.05$.

RESULTS

Correlations with Patient's Basic Characteristics

We found a linear, positive correlation between the patient age at scan and the $\bar{\chi}_{patient}$ ($p<0.05$, Figure 1), suggesting that older lesions have a higher iron concentration. The average change in $\bar{\chi}_{patient}$ was small (estimated to be 4.8% per decade of life) that may imply

a slow, progressive iron deposition. $\bar{\chi}_{patient}$ was not significantly different between genders. Furthermore, there was no correlation between $\bar{\chi}_{patient}$ in symptomatic patients and years since initial symptoms onset.

Correlations with Clinical Features of the Disease

Sporadic and familial CCM, and Lesion volume—We did not find a significant difference in $\bar{\chi}_{patient}$ between sporadic and familial CCM patients. No correlation was found between $\bar{\chi}_{lesion}$ and lesion volume, indicating that lesional iron concentration is independent of lesion volume.

Hemorrhagic and Non-hemorrhagic Lesions—CCM lesions in both sporadic and familial cases with previous overt hemorrhages were found to have significantly higher iron concentrations. $\bar{\chi}_{lesion}$ in 26 lesions that previously bled at least once was significantly higher than that in lesions (n = 277) that had no history of prior CCM hemorrhages ($p < 0.05$, Figure 2a). The 95% confidence interval for the difference between patients with and without overt hemorrhage was [0.39 to 0.50]. This result suggests CCM lesions with prior symptomatic bleeds harbor more iron or iron-containing products.

The difference in $\bar{\chi}_{lesion}$ between hemorrhagic and non-hemorrhagic cases was more prominent in familial CCM cases ($p < 0.01$, Figure 2b). Considering lesions with prior hemorrhagic events as the true positive group and the remaining lesions as the true negative group in our data, we performed ROC analysis as a measure of the overall discriminative performance of QSM, that is, the overall ability to identify lesions with prior bleeds ahead of those without. The AUC (area under curve) was 0.83, suggesting QSM had a good accuracy in identifying a lesion's prior hemorrhages (Figure 2c).

When controlling for lesion volume, the difference in $\bar{\chi}_{lesion}$ was not significant between hemorrhagic and non-hemorrhagic lesions. This suggests that the effect of prior hemorrhages on lesional iron concentration is mediated, at least in part by lesion volume.

Longitudinal Changes in Lesional Susceptibility

Changes in $\bar{\chi}_{lesion}$ were small among 33 patients in the short term (mean ± standard deviation, 300 ± 125 days, median, 360 days). The bias for changes in mean susceptibility was −0.0003 [95% confidence interval, −0.06, 0.06]), shown in the Bland-Altman plot (Figure 2d). Among the 33 patients, lesions from 20 patients were clinically stable without historical symptoms (bias = −0.003, 95% CI=[−0.064, 0.058]); 5 patients had a CCM related hemorrhage within 6 months prior to the first QSM (bias = −0.015, 95% CI=[−0.033, 0.064]); and 8 patients had a CCM related hemorrhage older than 6 months prior to the first QSM (bias = 0.23, 95% CI=[−0.044, 0.075]). None of the patients experienced a hemorrhage between their first and second QSM scan. In the same cohort, no significant correlation was found between changes in $\bar{\chi}_{lesion}$ and changes in lesion volume, indicating changes in lesional iron concentration can occur independently from changes in lesion volume.

Impact of Surgery and Recent Hemorrhage on QSM

In one sporadic patient (41 years old female), the lesion located in right frontal lobe was removed surgically prior to the second QSM scan. The success of the surgery was reflected on QSM image where only residual iron deposition was seen at the edge of the old lesion (Figure 3a).

One sporadic patient (28 years old female), in whom the CCM lesion bled 3 months before her first QSM scan in September, had a re-bleed in the same lesion in October. A second QSM scan was performed on her in December and an increase in both $\bar{\chi}_{\text{lesion}}$ (from 0.1751 ppm to 0.4659 ppm) and lesion volume (from 519 mm^3 to 932 mm^3) were observed (Figure 3b). We suspect the increase in lesional iron deposition is related to the two overt hemorrhages in such a short time frame. One other familial patient (2 years old male) had a hemorrhage 11 months after the first QSM scan with a second QSM follow-up 2 months later. However, no significant change was observed in the lesion that bled ($\bar{\chi}_{\text{lesion,1st QSM}}$=0.4966 ppm, 1st lesion volume = 3960 mm^3; $\bar{\chi}_{\text{lesion,2nd QSM}}$=0.4765 ppm, 2nd lesion volume = 3919 mm^3).

One other case worth noting was a 59 years old sporadic patient who had her first QSM scan 14 days after the lesion bled, and a second QSM scan was performed 35 days after. Although both the lesion volume and the total susceptibility decreased from 2165 mm^3 to 1242 mm^3 and 1130 ppm· mm^3 to 723 ppm· mm^3, respectively (Figure 3c), $\bar{\chi}_{\text{lesion}}$ increased slightly from 0.4298 ppm to 0.4791 ppm. This suggests the human body does not effectively remove the iron products associated with hemorrhage during the natural recovery progress. Furthermore, this case illustrates that changes in lesion volume do not necessarily reflect a concomitant changes in lesional iron concentration.

Overall, of the three cases with follow-up QSM after recent hemorrhages in longitudinal study, two had interval increase in lesional iron concentrations without increase in lesion volume, and a third had nearly 2.5 fold increase in lesional iron concentration, with only a 80% increase in lesion volume. This shows that increased iron concentration in CCM lesions can occur after hemorrhage, independent of lesion volume.

Spatial Correlation with Conventional MRIs

All CCM lesions revealed hypointense signal compared to normal brain parenchyma on QSM. A total of 41 ROIs were identified from 20 randomly selected CCM lesions, consisting of 9 DH, 8 ECM, 12 ICM, 7 hemosiderin, and 5 unknown regions. The signal intensities for DH, ECM, and ICM spanned the full spectrum (low to high) on the QSM images, whereas hemosiderin exhibited medium and high intensities, and the unidentified regions exhibited low intensities (Figure 4a). In particular, hemosiderin demonstrated most homogenous signal distribution on QSM, while the other blood byproduct regions exhibited both homogenous and heterogeneous signal distributions. An example of the spatial correlation between QSM and the conventional T1 and T2 images is shown in Figure 4b.

DISCUSSION

Our previous investigation [12] demonstrated the proof of concept that QSM can quantify lesional iron deposition in CCM. In the current study, we aim to evaluate the relationship between iron burden using QSM and the clinical features of the CCM disease in a larger clinical population.

Since the total iron content measured by QSM in CCM lesions is inherently related to the lesion size (i.e. larger lesion contains more iron deposition [12]), we sought to assess lesional mean susceptibility, a measurement proportional to the lesional iron concentration, as the metric to assess lesional iron burden. The results have confirmed the hypothesis that lesions in older patients had higher iron burden. We used age at scan as an estimate for the duration of lesion presence since lesion gensis is unknowlable in most cases. Other studies have analyzed bleed risk and other natural history features based on similar year of exposure since birth [3, 20]. Aging itself may be a factor for this observation given the increasing evidence to show older brains are associated with increased iron [21]. This observation supports the conservation of mass hypothesis, with QSM signal reflecting lesional permeability as demonstrated in a previous study [18], now reflected also by iron accumulation over time.

No correlation was found between lesional iron concentration and lesion volume. This finding confirmed our initial observation in the prior feasibility study [12]. Changes in lesional volume and iron concentration may be two independent indicators of different aspects of disease activities, which will be furthered examined in a future prospectively longitudinal investigation.

We found lesions with prior overt hemorrhages were shown to have a higher iron concentration than those without. Even though the observation was predominate in familial cases, it still indicates hemorrhages were related to iron depositions within CCM lesions, and confirmed that the human body lacks of an effective mechanism to clear out the residual iron products from a CCM during recovery. The ROC analysis suggests QSM might identify prior bleeding events in familial cases with a good sensitivity measure. This aspect of the QSM application is important, especially when data on patient's medical history is unknown or when patients do not present for medical evaluation after unknowingly experiencing a hemorrhage. While the mean iron concentration in bled lesions was higher than ones without bleeds in sporadic cases, it did not reach a statistical significance. This outcome may be related to the small sample size of sporadic bleeds.

Our cross-sectional data showed the hemorrhagic effect on the lesional iron concentration was mediated, at least in part, by lesion volume in cross sectional observations. This cohort may not have included sufficient number of hemorrhagic cases in all volume strata. Our data from the longitudinal study in patients with repeated QSM scans after recent hemorrhage showed manifested increase in lesional iron concentrations independent of lesional volume. To fully evaluate whether QSM offers an added measure beyond lesion size, a higher number of hemorrhagic patients with repeated scans is required.

The longitudinal results in cases with repeat QSM studies revealed little temporal change in lesional iron concentration during a period of up to 15 months in clinically stable lesions

(Figure 2d). Lesions included in the analysis consist of lesions without any prior hemorrhages, and those with prior hemorrhage in the chronic stage before the first QSM. In both scenarios, the susceptibility signal within the lesion remained relatively unchanged at short-term follow-up. The observation of minimum change in stable CCM lesions and increased susceptibility signal associated with overt hemorrhages may indicate that lesional iron concentration increases only in the presence of recent bleeds. This hypothesis will be subjected to more rigorous testing in a larger longitudinal study.

We found there was a large variation (estimated range of 0.4 – 1.9ppm) in the susceptibility signal within regions of different blood breakdown products (e.g. DH, ICM, ECM). Hemosiderin, however, consistently exhibited a higher mean susceptibility value (> 1.0 ppm). This could be a result of hemosiderin crystallization generating superparamagnetism [22]. The heterogeneity and variation of susceptibility values in DH, ICM, and ECM suggest there might be other contributing susceptibility sources. Overall, we believe the spatial distribution of the lesional susceptibility does offer additional information beyond the conventional MRIs, the details of which require further investigation.

Limitations of this study include lesional iron content that may be underestimated due to partial volume effects, since other susceptibility sources such as diamagnetic myelin were not accounted for. This study was not powered to detect the effects of lesional iron content in patients recovering from or with recent bleeds, although the ongoing study is currently accumulating additional data to power future studies in relation to ongoing CCM lesion activity. The classification of blood byproducts based on Bradley et. al. [19] was overly simplified. Differentiating various blood products was a difficult task and some ROIs regions contained spatially heterogeneous signal distribution on the conventional MRIs. Those regions were likely to contain a variety of blood iron products and they were classified according to the predominant signal appearances. In addition, we did not specifically examine CCM cases associated with seizures, where QSM may reflect lesional epileptogenicity, and this will be addressed in future studies. While the data in this study was not enough to establish a clinical utility for QSM, we postulate that QSM may be still used as a potential imaging biomarker to supplement information from conventional imaging, and to calibrate experimental therapies in future clinical trials targeted at reducing lesional iron deposition in CCM.

Summary

We demonstrated in the current study that: 1) lesional mean susceptibility was positively correlated with patient age; 2) lesions with prior symptomatic bleeding have higher mean susceptibility than those without; 3) changes in lesional susceptibility were minimal in clinically stable CCM lesions. Additionally, in a limited number of observations, there was significant increase in lesional mean susceptibility in association with new clinical hemorrhage, motivating further prospectively longitudinal investigation already underway. The findings in this study will be hypothesis-generating for future investigations that will help guide and design of human trials for potential treatments.

Supplementary Material

Refer to Web version on PubMed Central for supplementary material.

Acknowledgments

The project was funded in part by the Collaborative and Translational Studies Award through the Institute of Translational Medicine at the University of Chicago (*UL1 TR000430*) and by the Bill and Judy Davis Research Fund in Neurovascular Research. The authors thank Eugene Dunkle and Dr. Wei Li for assisting with data collection, and the Center for Advanced Imaging at NorthShore University HealthSystem for providing the scanning time and equipment for the study.

Funding:

This project was funded in part by the Collaborative and Translational Studies Award through the Institute of Translational Medicine at the University of Chicago (*UL1 TR000430*) and the Bill and Judy Davis Research Fund in Neurovascular Research.

ABBREVIATIONS

CCM	Cerebral Cavernous Malformations
SWI	Susceptibility Weighted Imaging
QSM	Quantitative Susceptibility Mapping
UC	University of Chicago
NSUHS	NorthShore University HealthSystem
GRE	Gradient Echo
ROI	Regions of Interests
DH	Deoxygenated Hemoglobin
ICM/ECM	Intra/Extra Cellular Methemoglobin
ppm	Parts Per Million
ROC	Receiver Operating Characteristics

References

1. Barrow, D.; Krisht, A. Cavernous malformation and hemorrhage. In: Awad, IA.; Barrow, D., editors. Cavernous Malformations. Park Ridge: American Association of Neurological Surgeons; 1993. p. 65-80.
2. Bruner, JM.; Tien, RD.; McLendon, RE. Tumors of vascular origin. In: Bigner, DD.; McLendon, RE.; Bruner, JM., editors. Russell and Rubinstein's Pathology of Tumors of the Nervous System. London: Arnold; 1998. p. 239-293.
3. Robinson JR, Awad IA, Little JR. Natural history of the cavernous angioma. J Neurosurg. 1991; 75:709–714. [PubMed: 1919692]
4. Robinson JR Jr, Awad IA, Magdinec M, et al. Factors predisposing to clinical disability in patients with cavernous malformations of the brain. Neurosurgery. 1993; 32:730–735. discussion 735–736. [PubMed: 8492847]

5. McDonald DA, Shenkar R, Shi C, et al. A novel mouse model of cerebral cavernous malformations based on the two-hit mutation hypothesis recapitulates the human disease. Hum Mol Genet. 2011; 20:211–222. [PubMed: 20940147]
6. McDonald DA, Shi C, Shenkar R, et al. Fasudil decreases lesion burden in a murine model of cerebral cavernous malformation disease. Stroke. 2012; 43:571–574. [PubMed: 22034008]
7. Shenkar R, Venkatasubramanian PN, Zhao JC, et al. Advanced magnetic resonance imaging of cerebral cavernous malformations: part I. High-field imaging of excised human lesions. Neurosurgery. 2008; 63:782–789. discussion 789. [PubMed: 18981890]
8. Haacke EM. Susceptibility weighted imaging (SWI). Z Med Phys. 2006; 16:237. [PubMed: 17216748]
9. de Champfleur NM, Langlois C, Ankenbrandt WJ, et al. Magnetic resonance imaging evaluation of cerebral cavernous malformations with susceptibility-weighted imaging. Neurosurgery. 2011; 68:641–647. discussion 647–648. [PubMed: 21164377]
10. Liu T, Liu J, de Rochefort L, et al. Morphology enabled dipole inversion (MEDI) from a single-angle acquisition: comparison with COSMOS in human brain imaging. Magn Reson Med. 2011; 66:777–783. [PubMed: 21465541]
11. Schweser F, Deistung A, Lehr BW, et al. Quantitative imaging of intrinsic magnetic tissue properties using MRI signal phase: an approach to in vivo brain iron metabolism? Neuroimage. 2011; 54:2789–2807. [PubMed: 21040794]
12. Tan H, Liu T, Wu Y, et al. Evaluation of iron content in human cerebral cavernous malformation using quantitative susceptibility mapping. Invest Radiol. 2014; 49:498–504. [PubMed: 24619210]
13. Liu T, Wisnieff C, Lou M, et al. Nonlinear formulation of the magnetic field to source relationship for robust quantitative susceptibility mapping. Magn Reson Med. 2013; 69:467–476. [PubMed: 22488774]
14. Liu T, Khalidov I, de Rochefort L, et al. A novel background field removal method for MRI using projection onto dipole fields (PDF). NMR Biomed. 2011; 24:1129–1136. [PubMed: 21387445]
15. Al-Shahi Salman R, Berg MJ, Morrison L, et al. Hemorrhage from cavernous malformations of the brain: definition and reporting standards. Angioma Alliance Scientific Advisory Board. Stroke. 2008; 39:3222–3230. [PubMed: 18974380]
16. Abdulrauf SI, Kaynar MY, Awad IA. A comparison of the clinical profile of cavernous malformations with and without associated venous malformations. Neurosurgery. 1999; 44:41–46. discussion 46–47. [PubMed: 9894962]
17. Campbell PG, Jabbour P, Yadla S, et al. Emerging clinical imaging techniques for cerebral cavernous malformations: a systematic review. Neurosurgical focus. 2010; 29:E6. [PubMed: 20809764]
18. Mikati AG, Tan H, Shenkar R, et al. Dynamic Permeability and Quantitative Susceptibility: Related Imaging Biomarkers in Cerebral Cavernous Malformations. Stroke. 2013
19. Bradley WG Jr. MR appearance of hemorrhage in the brain. Radiology. 1993; 189:15–26. [PubMed: 8372185]
20. Shenkar R, Shi C, Rebeiz T, et al. Exceptional aggressiveness of cerebral cavernous malformation disease associated with PDCD10 mutations. Genetics in medicine : official journal of the American College of Medical Genetics. 2015; 17:188–196. [PubMed: 25122144]
21. Zecca L, Youdim MB, Riederer P, et al. Iron, brain ageing and neurodegenerative disorders. Nature reviews Neuroscience. 2004; 5:863–873. [PubMed: 15496864]
22. Richter GW. Electron microscopy of hemosiderin; presence of ferritin and occurrence of crystalline lattices in hemosiderin deposits. The Journal of biophysical and biochemical cytology. 1958; 4:55–58. [PubMed: 13502428]

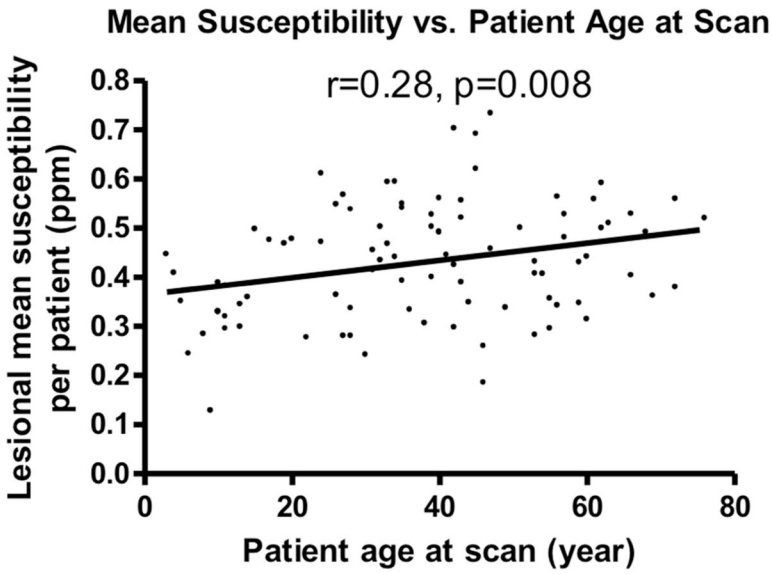

Figure 1.
Mean lesional susceptibility per patient (ppm) is positively correlated with patient age at scan.

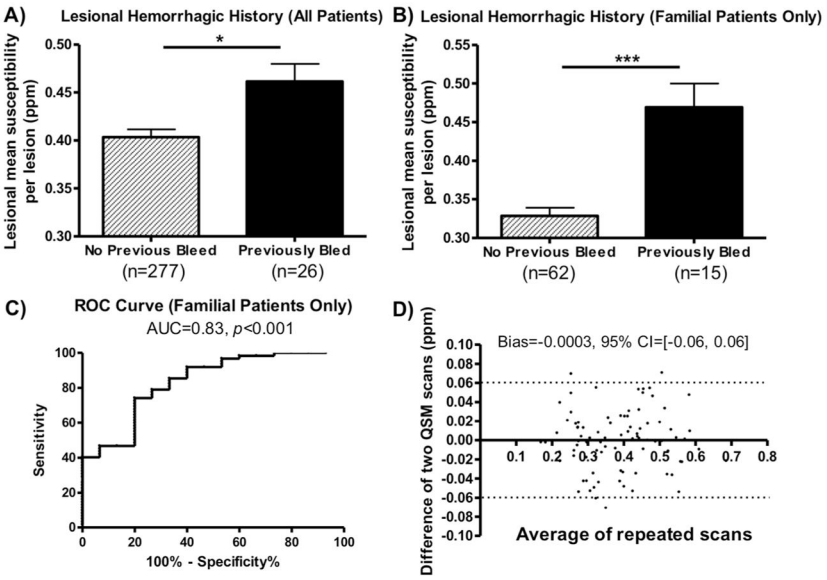

Figure 2.

A) Mean susceptibility comparison between lesions with and without prior hemorrhages in all patients. B) Mean susceptibility comparison between lesions with and without prior hemorrhages in only familial patients. C) ROC analysis indicates QSM is a good differentiator between lesions with and without prior hemorrhage in familial cases. D) Bland-Altman plot of the repeated QSM measurements. Changes in susceptibility were small in clinically stable patients within a short follow-up period.

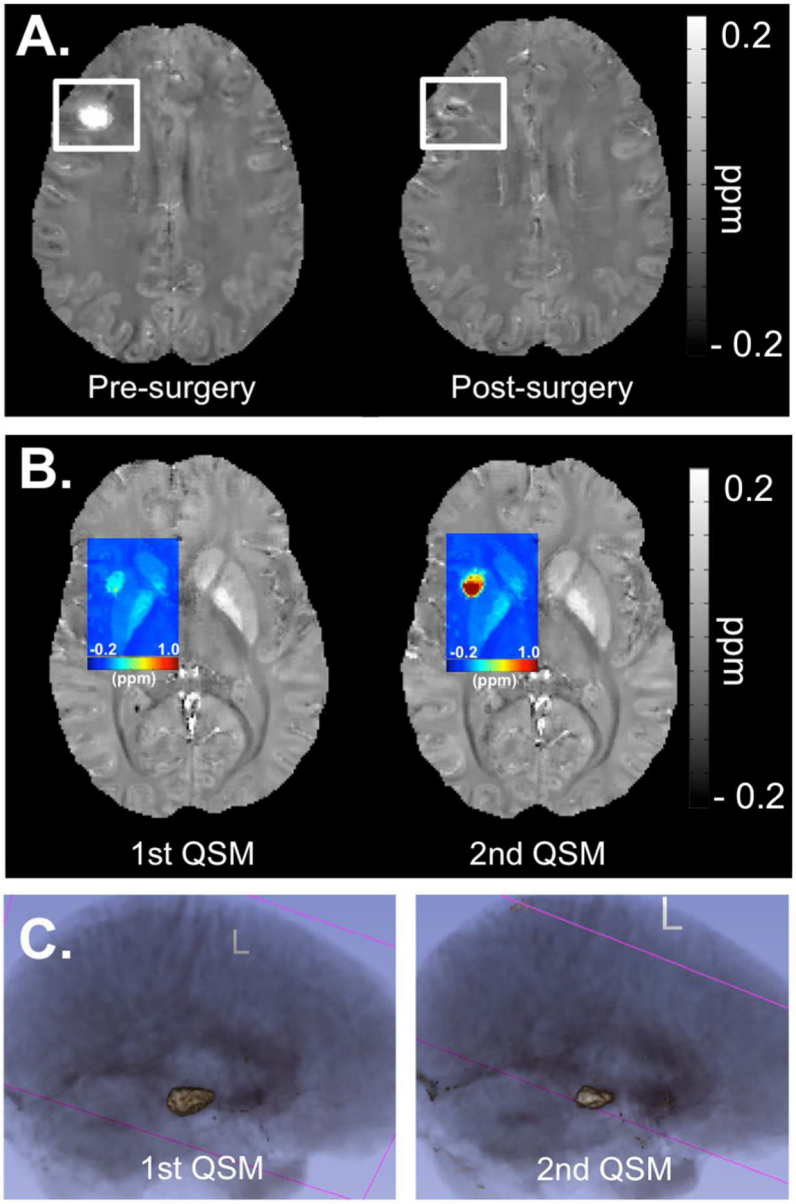

Figure 3.

Each subfigure exhibits a separate CCM case: A) QSM map depicting the appearance of a CCM lesion before and after surgery in a patient. B) Colorized QSM map depicting a big increase in iron deposition in the same CCM lesion in a short time, after two recent overt hemorrhages. C). 3D rendering of a CCM lesion in repeated scans after a known hemorrhage, depicting the shrinkage in overall lesion volume during the shortterm recovery period in a patient following a hemorrhage, but increased mean susceptibility.

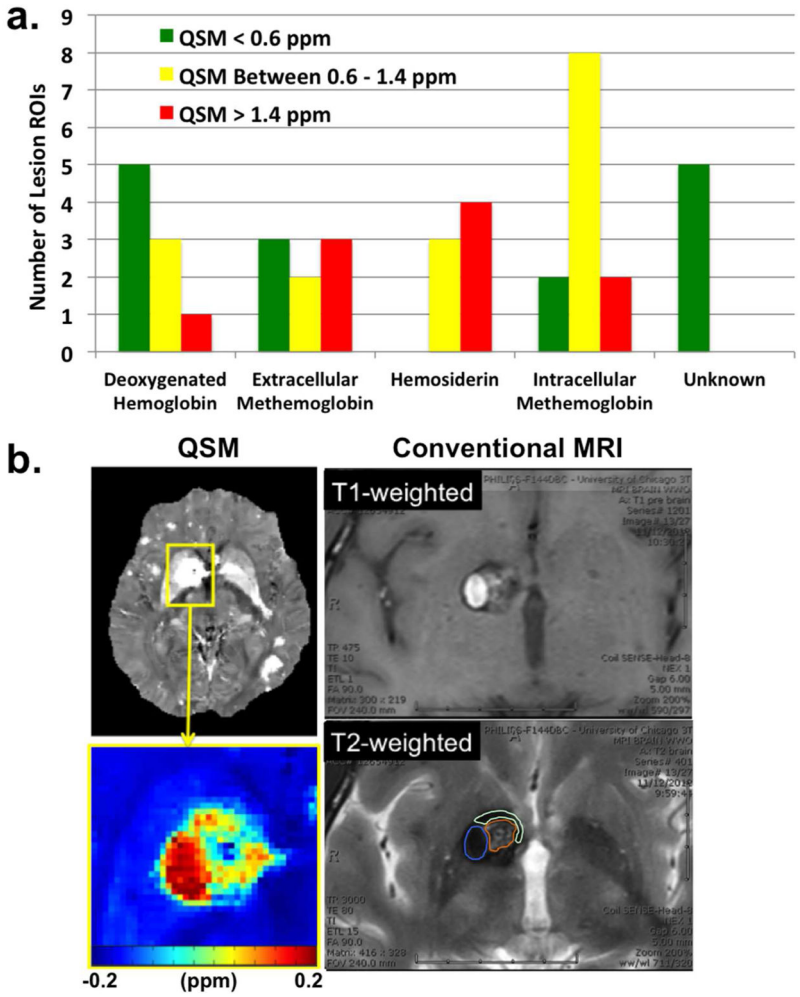

Figure 4.

Spatial comparison results between QSM and conventional MRI. (a) Susceptibility distribution of different blood breakdown byproducts within CCM lesions. (b). Illustration of blood breakdown byproduct identification and correlation with the corresponding QSM measurements. ROIs for different blood byproducts are shown in the T2-weighted image with color (blue – intracellular methemoglobin, brown – intracellular methemoglobin and hemosiderin, cyan – hemosiderin).

Table 1

Clinical information of the included patients.

Number of patients included in analysis	95
Mean age at first scan / range	40 / 3 – 76
Male / female	34 / 61
Number of sporadic / familial cases	39 / 56